Available online at www.sciencedirect.com
SCIENCE DIRECT®
Journal of Magnetic Resonance 166 (2004) 82–91
JMR Journal of Magnetic Resonance
www.elsevier.com/locate/jmr

Free radical EPR spectroscopy analysis using blind source separation

J.Y. Ren,[a] C.Q. Chang,[a] P.C.W. Fung,[b] J.G. Shen,[b] and F.H.Y. Chan[a,*]

[a] *Department of Electrical and Electronic Engineering, The University of Hong Kong, Hong Kong*
[b] *Department of Medicine, The University of Hong Kong, Hong Kong*

Received 17 July 2003; revised 14 October 2003

Abstract

In this paper, we propose a novel approach for electron paramagnetic resonance (EPR) mixture spectra analysis based on blind source separation (BSS) technique. EPR spectrum of a free radical is often superimposed by overlapping spectra of other species. It is important and challenging to accurately identify and quantify the 'pure' spectra from such mixtures. In this study, an automated BSS method implementing independent component analysis is used to extract the components from mixed EPR spectra that contain overlapping components of different paramagnetic centers. To apply this method, there is no requirement to know the component spectra or the number of components in advance. The method is applied to analyze free radical EPR spectra which are collected from standard chemical system, cultured cell suspense, and ex vivo rat kidneys by spin trapping EPR technique. Results show that the BSS method proposed here is capable of identifying the component EPR spectra from mixtures with unknown compositions. The BSS technique can offer powerful aids in resolving spectral overlapping problems in general EPR spectroscopy analysis.

Keywords: Electron paramagnetic resonance; Spectroscopy analysis; Blind source separation; Free radical; Independent component analysis

1. Introduction

Electron paramagnetic resonance (EPR) spectroscopy is a technique to detect the presence of unpaired electrons in biological samples. It has distinct advantage in many medical applications, especially for the direct measurement of free radicals which hold unpaired electrons [1], as free radicals play an important role in many physiological and pathophysiological pathways [2–4]. The detection of organic free radicals is difficult because of their low concentration and exceptionally short half-life properties. Furthermore, in many practical cases, it is common that more than one kind of free radical are involved in the EPR detection and hence the detected signal may be composed of a number of overlapping spectra, which gives rise to difficulty in quantitative analysis of the signal [5,6].

As free radicals are too highly reactive to detect directly, the spin trapping technique has been developed since the late 1960s [7–9], and has made remarkable contributions to identify various free radicals over decades of development [10–12]. The above stated difficulty has hence been mitigated by spin trapping techniques, but not eliminated. For example, the spin trap agent 5-(diethoxyphosphoryl)-5-methyl-1-pyrroline-*N*-oxide (DEPMPO) has been widely used to trap superoxide ($O_2^{-\cdot}$) radical in biological systems. However, DEPMPO simultaneously traps hydroxyl radical ($OH^{\cdot}$) in in vivo systems. The measured spectrum of superoxide–DEPMPO adduct is thus often superimposed on the spectrum of the hydroxyl–DEPMPO adduct. A similar problem also exists in nitric oxide (NO) measurement by spin trapping EPR spectroscopy, where the copper-adduct spectrum may contaminate the signal of the NO-adduct [13].

To identify pure spectra of free radicals from their mixtures measured by spin trapping EPR technique, traditional method usually proceeds by manually matching the mixtures with the reference spectra. This effort is apparently inefficient and highly dependent on the content of the reference spectra. Another approach was reported to determine the paramagnetic species from mixtures by determining the power saturation behavior of different spectral features [14]. However it is only applicable for limited species and a multitude of demanding experiments are required. Consequently, it is

* Corresponding author. Fax: +852-2559-8738.
E-mail address: fhychan@eee.hku.hk (F.H.Y. Chan).

1090-7807/$ - see front matter © 2003 Elsevier Inc. All rights reserved.
doi:10.1016/j.jmr.2003.10.015

desirable to develop a simple and generic method, which is not dependent on the reference spectra, for most EPR mixture spectra analysis. It is ideal if we can obtain pure component spectra from bulk spectra mixture numerically, though it has been proven challenging in EPR signal analysis [15]. To solve the problem, Steinbock et al. [16] have proposed an approach using principal component analysis (PCA), which has many applications in spectroscopy analysis such as in [17], combined with the self-modeling method or a method exploiting the symmetric feature of EPR spectra. The complexity of this approach, however, remarkably increases with the increase of the total number of components.

In this study, we introduce a blind source separation (BSS) method based on independent component analysis (ICA) to EPR spectra separation. BSS has found applications in many practical problems such as speech recognition [18], EEG analysis [19,20], functional magnetic resonance imaging (fMRI) [21], and NMR spectroscopy [22]. In this paper, the novel application of BSS method to EPR spectral analysis is proposed. Via the BSS method, we can estimate the source components from mixed EPR spectra even without the prior knowledge of the source components. That is, if a sufficient number of mixture spectra are recorded over a magnetic field interval, we can separate the components without knowing the source component spectra and the number of components in advance.

Using this species free method, we attempted to identify the pure sources from the observed overlapping EPR spectral mixtures as well as to estimate the percentages of the pure components contained in the mixtures. To test the validity of this method, references were chosen to be the well-characterized spectra of superoxide–DEPMPO and hydroxyl–DEPMPO adducts, which were produced from standard chemical systems. The simulated overlapping spectra were employed for mixture spectra separation. Also, we applied the proposed technique to analyze biological EPR spectra containing two and three kinds of overlapped signals, respectively.

2. Blind source separation of free radical EPR spectra

2.1. Mathematical model for blind source separation method

Blind source separation can be illustrated as in Fig. 1. We have access only to the mixtures $\mathbf{x}(n) = [x_1(n)x_2(n)\cdots x_M(n)]^{\mathrm{T}}$, which is assumed to be generated from a linear instantaneous mixing system as

$$\mathbf{x}(n) = \mathbf{A}\mathbf{s}(n) = \begin{bmatrix} a_{11} & a_{12} & \cdots & a_{1N} \\ a_{21} & a_{22} & \cdots & a_{2N} \\ \vdots & \vdots & \ddots & \vdots \\ a_{M1} & a_{M2} & \cdots & a_{MN} \end{bmatrix} \begin{bmatrix} s_1(n) \\ s_2(n) \\ \vdots \\ s_N(n) \end{bmatrix}, \quad (1)$$

where $\mathbf{A}$ is often defined as the mixing matrix, and $\mathbf{s}(n)$ are the source signals. This in fact means that, in the BSS model for EPR spectra analysis, the observed spectrum is assumed to be a linear superposition of the source components according to the principle of superposition. Our aim is to extract the source signals $\mathbf{s}(n)$ from the mixtures $\mathbf{x}(n)$, the only known data. This is equivalent to estimate a separating matrix $\mathbf{B}$, so that

$$\begin{aligned} \mathbf{y}(n) = \mathbf{B}\mathbf{x}(n) &= \begin{bmatrix} b_{11} & b_{12} & \cdots & b_{1M} \\ b_{21} & b_{22} & \cdots & b_{2M} \\ \vdots & \vdots & \ddots & \vdots \\ b_{N1} & b_{N2} & \cdots & b_{NM} \end{bmatrix} \begin{bmatrix} x_1(n) \\ x_2(n) \\ \vdots \\ x_M(n) \end{bmatrix} \\ &= \mathbf{P}\mathbf{s}(n) = \begin{bmatrix} p_1 s_1(n) \\ p_2 s_2(n) \\ \vdots \\ p_N s_N(n) \end{bmatrix}, \end{aligned} \quad (2)$$

where $\mathbf{P}$ is a permutation matrix that has one and only one non-zero element in each row and column. That is, the estimated vector signal $\mathbf{y}(n)$ contains a scaled form of all the original source signals with an undetermined order.

Further statistical assumption on the source signals is necessary to make the blind source separation problem solvable. The number of observed mixture signals should not be less than the number of source signals, i.e., $M \geqslant N$ in Eq. (1). If the statistical distributions of the sources are non-Gaussian (or at most one source is Gaussian) and mutually independent, ICA is a solution [23,24]. In another case where the sources are mutually and temporally uncorrelated, uncorrelated component analysis (UCA) is an alternative solution [25]. There are several algorithms in the literature to implement ICA [23,26] and UCA [25,27]. In our study, we use an algorithm called FastICA [26] to implement ICA. A program about this algorithm is also provided by Hurri et al. [28]. The program is implemented in MATLAB programming language.

In the FastICA method, the problem of estimating $\mathbf{B}$ is solved by maximizing the non-Gaussianity of $\mathbf{B}^{\mathrm{T}}\mathbf{x}$ to

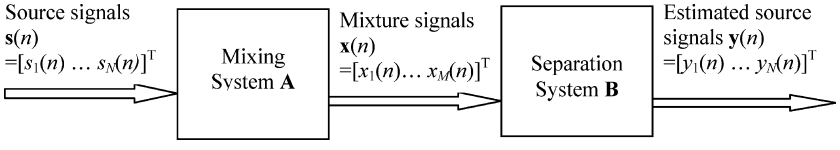

Fig. 1. The model of blind source separation method.

give a good approximation of **B** [26]. Based on this theory, the negentropy approximation function

$$J(\mathbf{B}^{\mathrm{T}}\mathbf{x}) \propto [E\{G(\mathbf{B}^{\mathrm{T}}\mathbf{x})\} - E\{G(v)\}]^2 \tag{3}$$

is used to construct a measure of non-Gaussianity, i.e., objective function for ICA estimation, where E is the expectation function, G is practically any non-quadratic function, and v is a Gaussian variable of zero mean and unit variance. By choosing G properly, one can obtain a suitable approximation of negentropy for a specific application. There are three forms of optimal G function in terms of asymptotic variance, robustness, and consistency in FastICA:

$$G_1(u) = \frac{1}{a_1}\log\cosh(a_1 u), \tag{4}$$

$$G_2(u) = -\frac{1}{a_2}\exp(-a_2 u^2/2), \tag{5}$$

$$G_3(u) = \frac{1}{4}u^4, \tag{6}$$

where $1 \leqslant a_1 \leqslant 2$, $a_2 \approx 1$ are constants. When the probability densities of the source data to be estimated are super-Gaussian (i.e., a density of positive kurtosis, indicating a relatively more peaked distribution than Gaussian), both G_1 and G_2 are suitable choices. Especially when the sources are highly super-Gaussian, or when robustness is very important, G_2 may be better. When the independent source components are sub-Gaussian (i.e., negative kurtosis density, with a relatively flat distribution), G_3 should be chosen.

2.2. Real problem of free radical EPR spectra and assumptions for BSS method

2.2.1. EPR spectra of superoxide and hydroxyl radical adduct

The typical EPR spectra of $O_2^{-}\cdot$ and OH· are shown in Figs. 2A and B in first derivative absorbance form, detected from standard chemical solution systems, and trapped by DEPMPO (see Section 5). Both spectra are basically octet lineshapes, but the detailed hyperfine structures are different due to the different nucleus–electron interactions. The resonance fields for both spectra are from 3420 to 3520 G at the frequency of about 9.75 GHz. In practical EPR detection of endogenous $O_2^{-}\cdot$ from Chinese hamster ovary (CHO) cell suspension (see Section 5), the spectra signals (Figs. 2C and D), however, are usually the combination of $O_2^{-}\cdot$ and OH· spectra embedded in high level noise. The corruption of the signals is mainly due to the fact that $O_2^{-}\cdot$ and OH· commonly coexist in cells and can both be trapped by DEPMPO. Peaks of both components in the spectra are heavily overlapped with each other leading to distorted component spectra. The individual components are thus difficult to identify and quantify. Therefore there is a need to employ BSS method to accurately and automatically separate and identify the components from the mixture spectra.

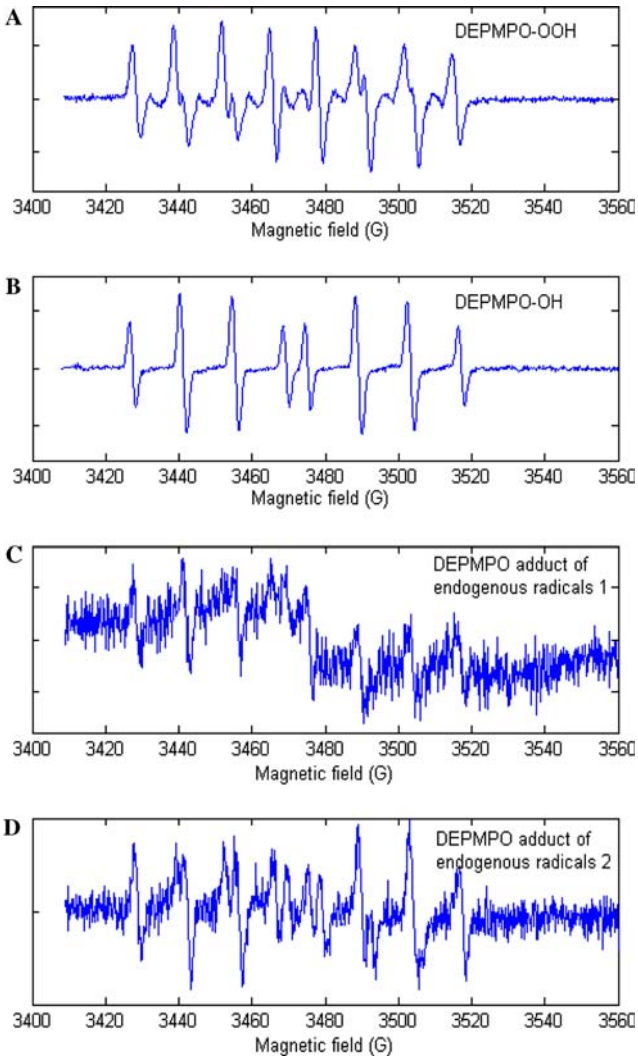

Fig. 2. (A) Typical EPR spectrum of $O_2^{-}\cdot$ adduct with DEPMPO of xanthine/xanthine oxidase chemical system. (B) Typical ERP spectrum of OH· adduct with DEPMPO of Fenton reaction system. (C,D) EPR signals of DEMPO adducts of Chinese hamster ovary cells with different processings. All signals of DEPMPO spin adduct were recorded with Bruker EMX EPR spectrometer. Representative spectroscopic parameters were: center field 3484 G, microwave frequency 9.76 GHz, microwave power 20 mW, modulation frequency 100 kHz, modulation amplitude 2 G, time constant 10 ms.

2.2.2. Assumptions for BSS analysis

In our BSS framework for free radical spectra analysis, we assume that several measurements of the free radical spectra can be obtained, with each measurement being a distinct linear superposition of the individual free radical spectrum. The assumption of linear superposition can be satisfied if no significant interactions occur between the free radicals (superoxide–DEPMPO and hydroxyl–DEPMPO adducts in our above exam-

ple), since this ensures that the individual EPR spectra are independently produced and hence the measured mixture spectrum is a simple linear superposition of the component spectra. By distinct superposition we mean that the ratios of these individual source spectra in one measurement are different from those in each other measurement. This can be automatically satisfied since, in most biological samples, different free radicals are present in different concentrations as well as their EPR signals increase or decay at different rates, which leads to variations in the component ratios in the recorded mixture spectra. It is not excluded, nevertheless, that in some cases a few components appear with constant proportion in all mixture spectra within a certain small error so that they may be estimated as one "pure" component. The number of measurements should be no less than the number of free radicals that can be measured. We further assume that the source radical spectra are statistically independent of each other and their statistical distributions are non-Gaussian. In practice, the assumption of statistical independence usually cannot be perfectly satisfied. However, approximate independence exists if the source free radical spectra are not overlapped or have one or more well separated lines. The ICA for the superimposed spectra can then give good estimates of source spectra for most of these cases. The non-Gaussian assumption means that the spectra data in our experiment should have a statistical distribution deviating from Gaussian (i.e., normal) distribution. The more deviation, the better separating results. Numerical analysis of the superoxide–DEPMPO spectrum and hydroxyl–DEPMPO spectrum shows that they are both non-Gaussian, more specifically, super-Gaussian as shown in Fig. 3. For super-Gaussian sources, we can use G1 or G2 in the FastICA algorithm. Analysis of other typical free radical spectra shows that most of them are statistically super-Gaussian.

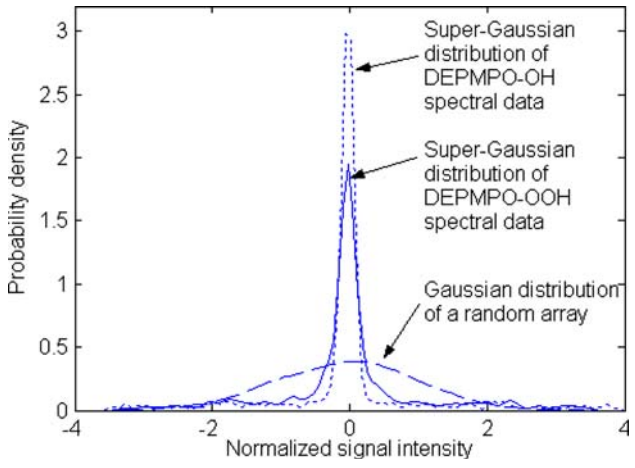

Fig. 3. Probability density estimate of DEPMPO–OH spectral data (dotted line) and DEPNPO–OOH spectral data (solid line), compared with Gaussian distribution (dashed line).

3. Results and discussions

The proposed BSS technique has been successfully tested in the simulated mixture spectra and applied to the spectra of biological samples. Here we show the results for simulations and two biological examples: (i) mixture spectra of superoxide and hydroxyl radicals of cellular systems and (ii) mixture spectra containing nitric oxide component which were obtained from ex vivo rat kidneys.

3.1. Blind source separation of simulated mixture spectra of superoxide and hydroxyl radical adducts

Experimental first-derivative lines of EPR spectra were directly employed for analysis. All the signal intensities were digitalized to 1024 equidistant points for further processing, and each spectrum was regarded as a 1024-dimensional vector. The spectra of superoxide–DEPMPO and hydroxyl–DEPMPO measured from chemical system are used as reference spectra. Overlapping complex spectra are simulated by mixing the reference spectra. By setting the mixing matrix with different values, a number of mixture spectra with different $O_2^{-}\cdot/OH\cdot$ ratios are acquired. Distinct superposition, required by our BSS approach, is thereby satisfied in the simulation.

Assuming the number of unknown components to be estimated is 2, which leads to the choice of '2' for the parameter 'numOfIC' in the FastICA program [28]. The number of mixtures provided for estimation is also 2 under the constraint $M \geqslant N$ as stated in Section 2.1. Sufficient number of combinations of two mixture spectra, containing overlapping components in different proportions, are formed for BSS application. One combination of the simulated mixture spectra for analysis is presented in Figs. 4A and B. Through estimating the probability density of pure superoxide–DEPMPO and hydroxyl–DEPMPO spectral data (Fig. 3), and computing kurtosis, one can find that both spectra samples have super-Gaussian statistical distribution. Therefore we choose G_1 to perform this method (refer to the mathematical model section). The parameter g (the derivative of G function) in the FastICA program is thereby set as 'tanh.' The parameters a_1 and a_2 are set as '1' in our implementation. After several iterations in implementing FastICA, the separating matrix **B** is quickly estimated, and thus two pure spectra are separated from the mixtures. The reconstructed source spectra are illustrated in Figs. 4C and D in solid lines. When one compares them with the dotted lines that represent the reference spectra, one can find only slight

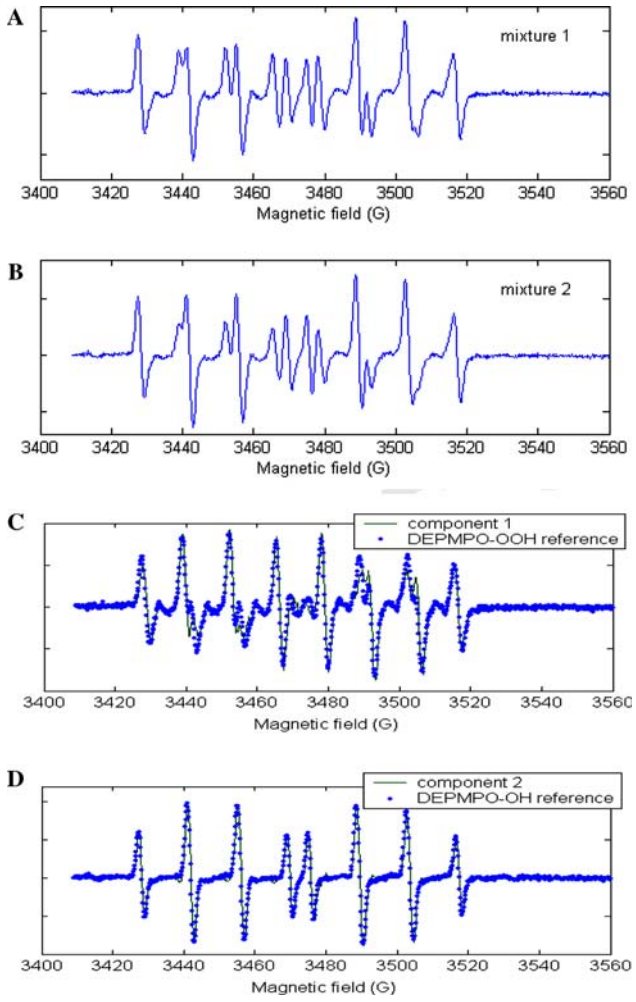

Fig. 4. (A,B) EPR signals of simulated mixture with signal amplitude ratios of $O_2^{-\cdot}$/OH· equal to 1/1 (A) and 1/1.75 (B), respectively. (C,D, solid lines) Retrieved source spectra from signals in (A,B) using BSS method with FastICA algorithm; (C,D, dotted lines) reference spectra of DEPMPO spin adducts of $O_2^{-\cdot}$ and OH·.

differences exist between the reconstructed spectra and the references.

To test the validity and stability of the suggested method for separating mixtures with various $O_2^{-\cdot}$/OH· ratios, we randomly set eight combinations of mixture spectra containing different proportions of $O_2^{-\cdot}$/OH· as shown in Table 1. After BSS application to each combination of mixture spectra, two source spectra were retrieved in each combination. Since the mixture spectra in each combination are combined of same sources of superoxide and hydroxyl adducts, the mathematically separated two spectra are expected to be same for each combination, and exhibit only the spectral lineshapes of superoxide–DEPMPO and hydroxyl–DEPMPO. In fact, it is the case for the practical application of BSS method to all combinations, as results show that the two separated spectra in each combination closely resemble the corresponding reference spectra.

The degree of similarity between theoretically retrieved spectra and reference spectra for each combination is measured by signal distortion index (SDI) as shown in Table 2. The SDI is defined as

$$\mathrm{SDI} = E[(\mathbf{r}-\mathbf{y})^2]/(E[\mathbf{r}^2]+E[\mathbf{y}^2]), \tag{7}$$

where E is the expectation function, $\mathbf{y}$ is the output of BSS, and $\mathbf{r}$ is the reference signal. The mean signal distortion index is 3.85% for superoxide–DEPMPO spectrum, and 0.26% for hydroxyl–DEPMPO spectrum. The signal distortion indexes are larger than 0 because the original spectra of superoxide–DEPMPO and hydroxyl–DEPMPO are not completely independent. Since the objective of ICA is to find the components as independent to each other as possible, but it is nearly impossible for the practical source components to be strictly statistically independent, there must be errors for the estimation. The more independent are the components, the more precise is the estimation. If the components are highly correlated, e.g., most peaks of one component are blurred by the peaks of other components, ICA method will not work well. In addition, the shape of the component spectrum is also important to the separation. Generally, spectra with sharp peaks tend to be well estimated like this example, since they tend to have quite peaked super-Gaussian distributions. When the spectral peaks are very broad and cause their distributions close to Gaussian, the estimate of the components, however,

Table 1
Signal amplitude ratios of $O_2^{-\cdot}$/OH· for different combinations of mixture spectra

Group No.	1	2	3	4	5	6	7	8
Mixture 1	1/1	1/1	1/1	1/1	1/1	3/1	3/1	3/1
Mixture 2	1/1.1	1/1.5	1/1.75	1/3	1/4	1/3	1/1.75	1/4

Table 2
SDI between separated spectra and reference spectra after blind source separation of the simulated mixture spectra

Group No.	1	2	3	4	5	6	7	8	Average
$O_2^{-\cdot}$	0.0388	0.0379	0.0407	0.0370	0.0381	0.0392	0.0350	0.0413	0.0385
OH·	0.0027	0.0029	0.0022	0.0036	0.0029	0.0021	0.0029	0.0018	0.0026

Table 3
Signal amplitude percentage (%) of true and estimated signals and their percentage difference for each simulated mixture spectra

Mixture No.	1	2	3	4	5	6	7	8	Average
True									
$O_2^{-}\cdot$	50	47.6	40	36.4	25	20	75	66.7	–
OH·	50	52.4	60	63.6	75	80	25	33.3	–
Estimated by BSS									
$O_2^{-}\cdot$	47.3	45.2	36.8	32.6	22.9	18.6	71.3	63.7	–
OH·	52.7	54.8	63.2	67.4	77.1	81.4	28.7	36.3	–
Percentage difference	2.7	2.4	3.2	3.8	2.1	1.4	3.7	3.0	2.8

will not be very satisfied. Nevertheless, the high consistence between reference and separated spectra shown by above data strongly indicates that the DEPMPO adduct spectra of superoxide and hydroxyl can be separated and reconstructed efficiently by BSS from their mixture signals.

The proposed method not only reveals the source spectra from the bulk mixture, it also allows us to conveniently estimate the percentages of hydroxyl radical and superoxide contained in the detected signals, which provides important aids in quantification analysis of free radical generation. The estimated amplitude percentage of each component in the mixture signal using this method is presented in Table 3. From these data one can find that, for each radical species, the difference between the true and the estimated percentage is only 2.8% on average, which suggests that the component percentages estimated using the method can be regarded as reliable information within a small error. As for the source of the error, it may mostly come from the fact that the statistical distributions of the two component spectra are not entirely independent with each other.

3.2. Application to EPR spectra obtained from biological samples

The procedures can be summarized as follows:

(a) EPR detection (usually use spin traps for measuring free radicals) of biological samples to obtain spectral data.
(b) Data alignment as preprocessing of data.
(c) Noise reduction of spectral signals.
(d) Implementation of blind source separation method to identify source spectra and estimate the proportion of the components.

Some parts that have not been previously stated will be highlighted as follows.

3.2.1. Data alignment

In EPR measurement, because microwave frequencies may be different among different recordings even for repeated measurements of the same paramagnetic centers, the spectra will shift with each other to some extent. Although the shift may not be significant, it severely hampers the mixture analysis. To cope with this problem, we compare each set of data using correlation analysis method. Since the mixture spectra in our analysis are combined of same components, the mixtures must have similar spectral features; thus they should be mostly correlated when they do not shift with each other. We first choose a signal as reference, then compute the correlation coefficient between the reference and each other spectrum, and finally move the spectrum vector of interest along the magnetic field axis to the place where the correlation coefficient value is the highest. Thereby the spectral shift factor can be eliminated through this preprocessing.

3.2.2. Application to real example: noise reduction and blind separation of overlapping spectra of cellular systems

In practical situations, it is common that EPR signals of biological samples suffer from the problem of very low signal-to-noise ratio (SNR) and baseline distortion which might be due to the instability of detecting condition during slow scan. Some filtering techniques, such as adaptive filtering [29,30], were applied to reduce noise for better performance of BSS. When a reference and a primary signal are fed into the filter, the adaptive filter compares the primary signal with the reference, and adjusts its own parameters until finally gives a minimum mean-square error estimate of the pure signal of interest that is contained in the primary noisy signal. In our implementation of filtering the primary noisy signals of CHO cells as shown in Figs. 5A and B, we employed the reference signals by averaging a set of similarly measured spectral signals. Figs. 5C and D illustrate the outputs of our adaptive filter. Then, the preprocessed mixture spectra underwent the processing of FastICA method, where the G function and other inputs of the implementation were chosen the same as in the simulation. The finally separated spectra are presented in Figs. 5E and F, solid lines. One can find that their peaks are quite discernible, and closely resemble the dotted lines in Figs. 5E and F that describe the corresponding reference spectra of superoxide–DEPMPO and hydroxyl–DEPMPO.

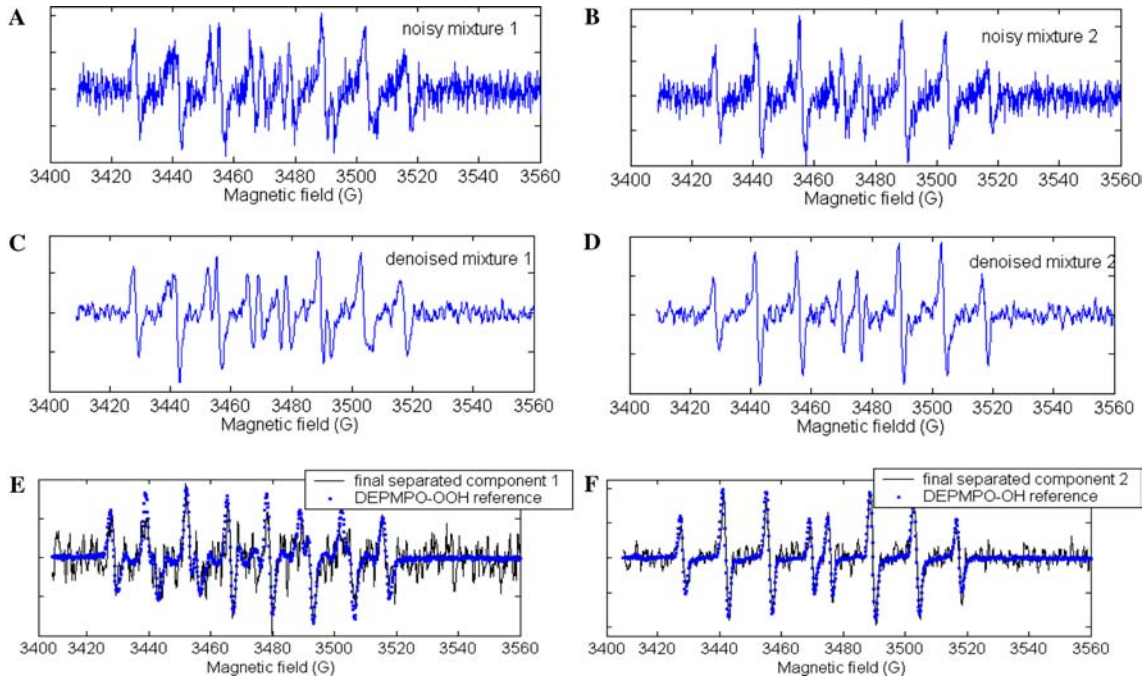

Fig. 5. (A,B) EPR signals of DEMPO adducts obtained from CHO cellular systems. The detecting conditions are as in Fig. 2. (C,D) Mixture signals filtered from noise corrupted signals in (A,B) using adaptive filtering method. (E,F, solid lines) Estimated source component spectra from mixtures in (C,D) using BSS method; (E,F, dotted lines) reference spectra of DEPMPO spin adduct of $O_2^{-}\cdot$ and $OH\cdot$.

In addition, in our simulation test with Gaussian noise added and using adaptive filtering technique for preprocessing, it has been found that the effectiveness of our BSS method increases with the elevation of SNR of primary mixture signals. When the SNR of primary mixture signal is set to 3, the distortion index between the separated $O_2^{-}\cdot$ signal and its reference can reach as small as 0.25, and the value is even smaller for $OH\cdot$ signal.

3.2.3. Demonstration of real example: identification of nitric oxide signal obtained from ex vivo rat kidneys

Spin trapping EPR spectroscopy is widely employed for unequivocal detection of NO in living systems, where DETC is used for trapping NO to form a stable adduct $DETC_2$–Fe^{2+}–NO. Forasmuch as the major problem due to superposition of manifold components also appears here, we have attempted to use BSS to estimate biological NO EPR signal. Figs. 6A–C exhibit the ex vivo EPR spectra detected from three rat kidneys that receive intraperitoneal injections of DETC 30 min before sacrifice (see Section 5). Because of the low concentration of NO, there is an increase in the binding of DETC to copper and a few other sources such as reduced iron–sulfur proteins, which results in complex background signal superimposed with NO EPR signal [13,31,32]. Therefore, the EPR signals of $DETC_2$–Fe^{2+}–NO present only doublet lines in Figs. 6A–C.

Since we can regard several components present in constant proportion as one "pure" component during BSS estimation, we assume there are three unknown components to be estimated, hence at least three detected mixture spectra with various component proportions should be provided for separation by BSS under the constraint $M \geqslant N$, as stated in Section 2.1. Considering the components are unknown in the mixture signal and the statistical distributions of most free radical spectra are super-Gaussian, the function $G_1(u) = 1/a_1 \log\cosh(a_1 u)$ is employed for this case. After the application of BSS to the mixture signals in Figs. 6A–C, the estimated component spectra are shown in Figs. 6D–F. Fig. 6D presents typical triplet lines which are the well-known characteristic spectrum of $DETC_2$–Fe^{2+}–NO. It reveals that, in the original recorded mixture signals, the pure spectrum of $DETC_2$–Fe^{2+}–NO was partially masked by Cu^{2+}–DETC signal. The presence of the spectrum in Fig. 6E is mainly due to the contribution of Cu^{2+}–DETC and reduced iron–sulfur proteins according to the computations of their g value. The fact that the spectra of the two components present together in this separated signal, suggests they are estimated as "one" compound by BSS method. It thereby indicates that the both compounds might appear in close concentration proportions in the kidney samples which are used for measurements. In Fig. 6F there is only noise remained because no other typical spectral lines can be figured out by BSS. After this procedure, the double integration of $DETC_2$–Fe^{2+}–NO spectra also becomes possible and allows a quantitative determination of $DETC_2$–Fe^{2+}–NO spectra in living

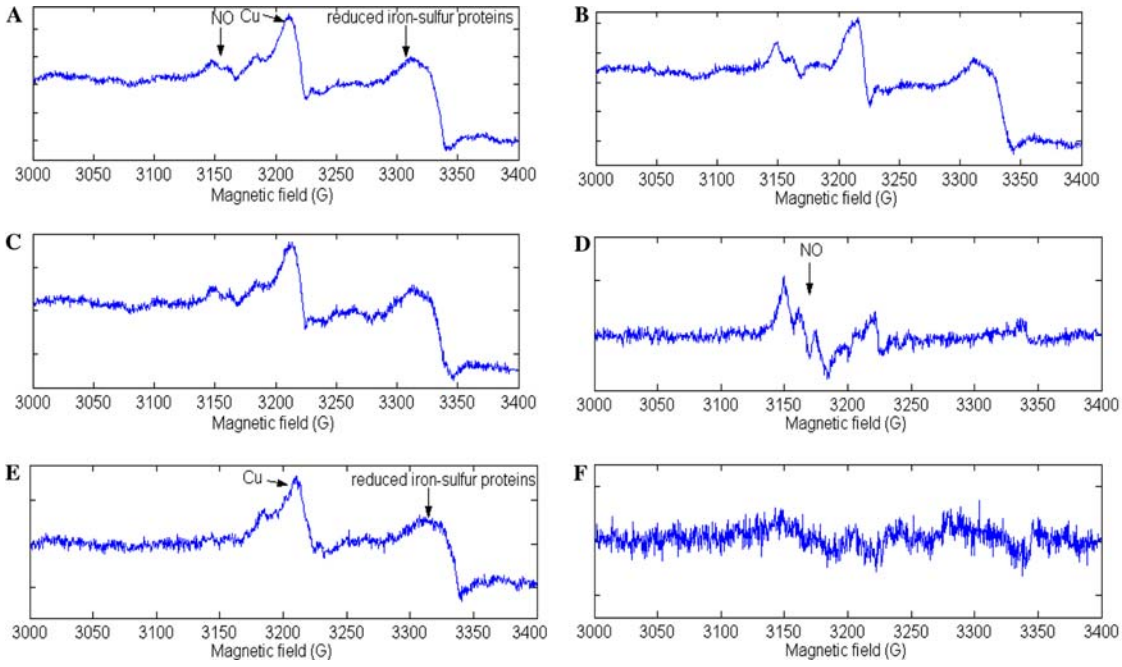

Fig. 6. (A–C) Typical EPR spectra of DETC spin adducts recorded from rat kidneys with different NO concentrations in the three figures. Two spin trapping agents, DETC, intraperitoneally, and iron citrate, subcutaneously, were administered to the rats 30 min before laparotomy. Signals were recorded at 77 K on a Bruker EPR 300E spectrometer operating at X-band with a microwave frequency about 9.45 GHz, 1.0 mW microwave power, and modulation amplitude of 5.19 G. (D,E,F) Retrieved source signals from the three observed spectral data in (A,B,C) using BSS method with FastICA algorithm. Especially, the spectrum in (D) closely resembles characteristic $DETC_2$–Fe^{2+}–NO signal, while the spectrum in (E) seems to be the combination of Cu^{2+}–DETC and reduced iron–sulfur proteins signals, only noise remains in (F).

animals even with abundant copper and other metal contents.

4. Conclusion

In this paper we present a study on evaluating the analytical potential of the BSS technique in EPR spectroscopy, since the phenomenon of spectral superposition of multiple components appears in many realistic spectra, leading to a major problem in analysis. A BSS method based on independent component analysis has been developed free of the features of the detected compounds (metals, free radicals, and so on). The merit of this method is that we can apply it even without knowledge of the source component signal and the way of mixing in advance. Using BSS, we can conveniently estimate the source spectra and their percentages in the total signal from a set of observed mixture spectra. To make the BSS based on ICA work well, there are constraints for the components such as the non-Gaussian distribution and the independence between them, though it does not require that the constraints be very strict. On the basis of the good agreement between different kinds of experimentally observed and theoretically retrieved spectra in our demonstration, we conclude that in the general EPR cases where the spectra are overlapped, the availability of a technique such as the one introduced here could be an important aid.

5. Experimental

5.1. Materials

Ham's F-12 medium and penicillin–streptomycin were purchased from Cellgro while fetal bovine serum (FBS) was bought from Gibco Life Technologies. Spin trapping reagent DEPMPO was purchased from Oxis International. Other chemicals were purchased from Sigma Chemical unless otherwise stated.

5.2. Standard chemical systems and generation of superoxide and hydroxyl radicals

Xanthine/xanthine oxidase system (Eq. (8)) to generate superoxide and Fenton reaction system (Eq. (9)) to generate hydroxyl radical were employed [33]

$$\text{Xanthine} + H_2O + 2O_2 \rightarrow \text{uric acid} + 2O_2^{-\cdot} + 2H^+ \quad (8)$$

$$Fe^{2+} + H_2O_2 \rightarrow Fe^{3+} + OH^- + OH^{\cdot} \quad (9)$$

The chemical system for $O_2^{-\cdot}$ production is composed with 0.32 mM xanthine, 9×10^{-3} unit/ml of xanthine oxidase, and 20 mM of DEPMPO in 1× PBS solution at

pH 7.4. The reaction system for $OH^{\cdot}$ production consists of 0.18 mM hydrogen peroxide, 0.09 mM $FeCl_2$ and 20 mM DEPMPO.

5.3. Cell culture and generation of superoxide and hydroxyl radicals

CHO cells were obtained originally from ATCC. The cells were grown as monolayers in Ham's F-12 medium supplemented with 10% fetal bovine serum (v/v) and 1% penicillin–streptomycin. The cells were cultured at 37 °C in an incubator supplemented with 95% air and 5% CO_2. A redox cycling reagent menadione sodium bisulfite (MSB) was introduced into the cultured media because of its solubility in water and its metabolism to semiquinone, yielding the parent quinone and superoxide, which may lead to the formation of other reactive oxygen species such as hydroxyl radicals and singlet oxygen [34]. As much as 50 μmol/L of MSB was used to induce the production of ROS in the CHO cells.

5.4. EPR spectroscopy and spin trapping of superoxide and hydroxyl radicals

For EPR spin trapping experiments, wild type CHO cells at a concentration of 5×10^6 cells/ml were incubated with 20 mM DEPMPO, 10% dextran, and 50 μmol/L menadione. The cell suspension was immediately drawn into a gas permeable Teflon tube and put into EPR cavity. The spectra of DEPMPO spin adduct were recorded with Bruker EMX EPR spectrometer. Representative spectroscopic parameters were: center field 3484 G, microwave frequency 9.76 GHz, microwave power 20 mW, modulation frequency 100 kHz, modulation amplitude 2 G, and time constant 10 ms. The spectrometer was interfaced with WinEPR for data acquisition in EPR experiments and handling of the spectra.

5.5. Measurement of nitric oxide radical in rats kidneys

Organic nitric oxide (NO) was also detected by spin trapping EPR method. Thirty minutes before the sacrifice, spin trap diethyldithiocarbamate (DETC) (Aldrich) 500 mg/kg were injected intraperitoneally, ferrous sulphate 50 mg/kg and sodium citrate 250 mg/kg were introduced subcutaneously at the same time. After laparotomy, left nephrotomy was performed and kidney tissue was carefully cut into small cylinders. Then the tissue was immediately put into EPR flat tube and placed in liquid nitrogen for EPR detection. Measurements were performed with an ESP 300E spectrometer (Bruker) operating at X-band, 77 K, microwave frequency about 9.75 GHz, magnetic field range from 3000 to 3400 G, microwave power 1.0 mW, and modulation amplitude of 5.19 G.

References

[1] L.J. Berliner (Ed.), In Vivo EPR (ESR): Theory and Applications, Biological Magnetic Resonance, vol. 18, Kluwer Academic/Plenum, New York, 2000.
[2] J.V. Bonventre, Mechanisms of ischemic acute renal failure, Kidney Int. 43 (1993) 1160–1178.
[3] J.G. Maessen, Reperfusion injury in the kidney, in: D.K. Das (Ed.), Pathophysiology of Reperfusion Injury, CRC Press, Boca Raton, FL, 1993, pp. 79–100.
[4] G.M. Rosen, B.E. Britigan, H.J. Halpern, S. Pou, Free Radicals: Biology and Detection by Spin Trapping, Oxford University Press, New York, 1999.
[5] T. Prisner, M. Rohrer, F. MacMillan, Pulsed EPR spectroscopy: biological applications, Annu. Rev. Phys. Chem. 52 (2001) 279–313.
[6] B. Kirste, Methods for automated analysis and simulation of electron paramagnetic resonance spectra, Anal. Chim. Acta 265 (1992) 191–200.
[7] G.R. Chalfont, M.J. Perkins, A. Horsfield, A probe for homolytic reactions in solution, J. Am. Chem. Soc. 90 (1968) 7141–7142.
[8] E.G. Janzen, B.J. Blackburn, Detection and identification of short-lived free radicals by an electron spin resonance trapping technique, J. Am. Chem. Soc. 90 (1968) 5909–5910.
[9] E.G. Janzen, Spin trapping, Acc. Chem. Res. 4 (1971) 31–40.
[10] K.J. Liu, M. Miyake, T. Panz, H. Swartz, Evaluation of DEPMPO as a spin trapping agent in biological systems, Free Radic. Biol. Med. 26 (1999) 714–721.
[11] L.J. Berliner, V. Khramtsov, H. Fujii, T.L. Clanton, Unique in vivo applications of spin traps, Free Radic. Biol. Med. 30 (2001) 489–499.
[12] T. Nagano, T. Yoshimura, Bioimaging of nitric oxide, Chem. Rev. 102 (2002) 1235–1270.
[13] L.N. Kubrina, W.S. Caldwell, P.I. Mordvintcev, I.V. Malenkova, A.F. Vanin, EPR evidence for nitric oxide production from guanidino nitrogens of L-arginine in animal tissues in vivo, Biochim. Biophys. Acta 1099 (1992) 233–237.
[14] D.E. Wilcox, R.P. Smith, Detection and quantification of nitric oxide using electron magnetic resonance spectroscopy, Methods 7 (1995) 59–70.
[15] D.A. Svistunenko, M.A. Sharpe, P. Nicholls, M.T. Wilson, C.E. Cooper, A new method for quantitation of spin concentration by EPR spectroscopy: application to methemoglobin and metmyoglobin, J. Magn. Reson. 142 (2000) 266–275.
[16] O. Steinbock, B. Neumann, B. Cage, J. Saltiel, S.C. Muller, N.S. Dalal, A demonstration of principal component analysis for EPR spectroscopy: identifying pure component spectra from complex spectra, Anal. Chem. 69 (1997) 3708–3713.
[17] R. Stoyanova, T.R. Brown, NMR spectral quantitation by principal component analysis. III. A generalized procedure for determination of lineshape variations, J. Magn. Reson. 154 (2002) 163–175.
[18] Z. Roth, Y. Baram, Multidimensional density shaping by sigmoids, IEEE Trans. Neural Netw. 7 (1996) 1291–1298.
[19] T.-P. Jung, C. Humphries, T.-W. Lee, S. Makeig, M. McKeown, V. Iragui, T. Sejnowski, Extended ICA removes artifacts from electroencephalographic recordings, in: M.I. Jordan, M.J. Kearns, S.A. Solla (Eds.), Advances in Neural Information Processing Systems, MIT Press, Cambridge, 1998, pp. 894–900.
[20] S. Makeig, A. Bell, T.-P. Jung, T. Sejnowski, Independent component analysis of electroencephalographic data, in: D.S. Touretzky, M.C. Mozer, M.E. Hasselmo (Eds.), Advances in Neural Information Processing Systems, MIT Press, Cambridge, 1996, pp. 145–151.

[21] M.J. McKeown, T.-P. Jung, S. Makeig, G. Brown, S.S. Kindermann, T.-W. Lee, T.J. Sejnowski, Spatially independent activity patterns in functional MRI data during the Stroop color-naming task, Proc. Natl. Acad. Sci. USA 95 (1998) 803–810.
[22] D. Nuzillard, S. Bourg, J.-M. Nuzillard, Model-free analysis of mixtures by NMR using blind source separation, J. Magn. Reson. 133 (1998) 358–363.
[23] P. Comon, Independent component analysis, a new concept, Signal Process. 36 (1994) 287–314.
[24] A. Hyvärinen, J. Karhunen, E. Oja, Independent Component Analysis, Wiley, New York, 2001.
[25] C.Q. Chang, S.F. Yau, P. Kwok, F.H.Y. Chan, F.K. Lam, Uncorrelated component analysis for blind source separation, Circuits Syst. Signal Process. 18 (1999) 225–239.
[26] A. Hyvärinen, Fast and robust fixed-point algorithms for independent component analysis, IEEE Trans. Neural Netw. 10 (1999) 626–634.
[27] C.Q. Chang, Z. Ding, S.F. Yau, F.H.Y. Chan, A matrix-pencil approach to blind separation of colored nonstationary signals, IEEE Trans. Signal Process. 48 (2000) 900–907.
[28] J. Hurri, H. Gävert, J. Särelä, A. Hyvärinen, Available from <http://www.cis.hut.fi/projects/ica/fastica>.
[29] F.H.Y. Chan, W. Qiu, F.K. Lam, P.W.F. Poon, M.K. Lam, Evoked potential estimation using modified time-sequenced adaptive filter, Med. Biol. Eng. Comput. 36 (1998) 407–414.
[30] W. Qiu, K.S.M. Fung, F.H.Y. Chan, F.K. Lam, P.W.F. Poon, R.P. Hamernik, Adaptive filtering of evoked potentials with radial-basis-function neural network prefilter, IEEE Trans. Biomed. Eng. 49 (2002) 225–232.
[31] W. Zhu, P.C. Fung, The roles played by crucial free radicals like lipid free radicals, nitric oxide, and enzymes NOS and NADPH in CCl(4)-induced acute liver injury of mice, Free. Radic. Biol. Med. 29 (2000) 870–880.
[32] J. Shen, J. Wang, B. Zhao, J. Hou, T. Gao, W. Xin, Effects of EGb 761 on nitric oxide and oxygen free radicals, myocardial damage and arrhythmia in ischemia–reperfusion injury in vivo, Biochim. Biophys. Acta 1406 (1998) 228–236.
[33] C. Frejaville, H. Karoui, B. Tuccio, F.L. Moigne, M. Culcasi, S. Pietri, 5-(Diethoxyphosphoryl)-5-methyl-1-pyrroline *N*-oxide: a new efficient phosphorylated nitrone for the in vitro and in vivo spin trapping of oxygen-centered radicals, J. Med. Chem. 38 (1995) 258–265.
[34] B.M. Hasspieler, R.T. Di Giulio, DT diaphorase [NAD(P)H: (quinone acceptor) oxidoreductase] facilitates redox cycling of menadione in channel catfish (*Ictalurus punctatus*) cytosol, Toxicol. Appl. Pharmacol. 114 (1992) 156–161.